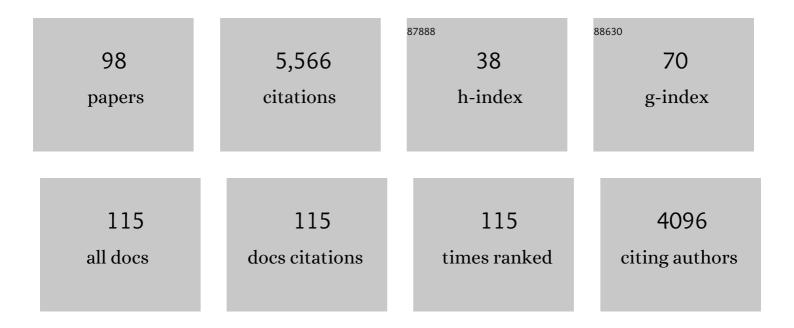
List of Publications by Year in descending order

Source: https://exaly.com/author-pdf/3236323/publications.pdf Version: 2024-02-01



5

#	Article	IF	CITATIONS
1	The SMOS Soil Moisture Retrieval Algorithm. IEEE Transactions on Geoscience and Remote Sensing, 2012, 50, 1384-1403.	6.3	793
2	Modelling the passive microwave signature from land surfaces: A review of recent results and application to the L-band SMOS & SMAP soil moisture retrieval algorithms. Remote Sensing of Environment, 2017, 192, 238-262.	11.0	323
3	Overview of SMOS performance in terms of global soil moisture monitoring after six years in operation. Remote Sensing of Environment, 2016, 180, 40-63.	11.0	240
4	Estimating maize biomass and yield over large areas using high spatial and temporal resolution Sentinel-2 like remote sensing data. Remote Sensing of Environment, 2016, 184, 668-681.	11.0	219
5	Evaluation of SMOS Soil Moisture Products Over Continental U.S. Using the SCAN/SNOTEL Network. IEEE Transactions on Geoscience and Remote Sensing, 2012, 50, 1572-1586.	6.3	218
6	Global-scale evaluation of two satellite-based passive microwave soil moisture datasets (SMOS and) Tj ETQq0 0 0 2014, 149, 181-195.	rgBT /Ove 11.0	erlock 10 Tf 202
7	SMOS-IC: An Alternative SMOS Soil Moisture and Vegetation Optical Depth Product. Remote Sensing, 2017, 9, 457.	4.0	195
8	Disaggregation of SMOS Soil Moisture in Southeastern Australia. IEEE Transactions on Geoscience and Remote Sensing, 2012, 50, 1556-1571.	6.3	185
9	SMOS soil moisture assimilation for improved hydrologic simulation in the Murray Darling Basin, Australia. Remote Sensing of Environment, 2015, 168, 146-162.	11.0	180
10	Self-calibrated evaporation-based disaggregation of SMOS soil moisture: An evaluation study at 3 km and 100 m resolution in Catalunya, Spain. Remote Sensing of Environment, 2013, 130, 25-38.	11.0	163
11	Global-scale comparison of passive (SMOS) and active (ASCAT) satellite based microwave soil moisture retrievals with soil moisture simulations (MERRA-Land). Remote Sensing of Environment, 2014, 152, 614-626.	11.0	160
12	The global SMOS LevelÂ3 daily soil moisture and brightness temperature maps. Earth System Science Data, 2017, 9, 293-315.	9.9	160
13	DART: Recent Advances in Remote Sensing Data Modeling With Atmosphere, Polarization, and Chlorophyll Fluorescence. IEEE Journal of Selected Topics in Applied Earth Observations and Remote Sensing, 2017, 10, 2640-2649.	4.9	146
14	An improved algorithm for disaggregating microwave-derived soil moisture based on red, near-infrared and thermal-infrared data. Remote Sensing of Environment, 2010, 114, 2305-2316.	11.0	127
15	SMOS disaggregated soil moisture product at 1 km resolution: Processor overview and first validation results. Remote Sensing of Environment, 2016, 180, 361-376.	11.0	112
16	First evaluation of the simultaneous SMOS and ELBARA-II observations in the Mediterranean region. Remote Sensing of Environment, 2012, 124, 26-37.	11.0	105
17	An evaluation of SMOS L-band vegetation optical depth (L-VOD) data sets: high sensitivity of L-VOD to above-ground biomass in Africa. Biogeosciences, 2018, 15, 4627-4645.	3.3	97
18	Evaluating soil moisture retrievals from ESA's SMOS and NASA's SMAP brightness temperature datasets. Remote Sensing of Environment, 2017, 193, 257-273.	11.0	90

#	Article	IF	CITATIONS
19	Comparison Between SMOS, VUA, ASCAT, and ECMWF Soil Moisture Products Over Four Watersheds in U.S IEEE Transactions on Geoscience and Remote Sensing, 2014, 52, 1562-1571.	6.3	88
20	Denitrification in wetlands: A review towards a quantification at global scale. Science of the Total Environment, 2021, 754, 142398.	8.0	77
21	Evaluation of microwave remote sensing for monitoring live fuel moisture content in the Mediterranean region. Remote Sensing of Environment, 2018, 205, 210-223.	11.0	75
22	Detection of Irrigated Crops from Sentinel-1 and Sentinel-2 Data to Estimate Seasonal Groundwater Use in South India. Remote Sensing, 2017, 9, 1119.	4.0	74
23	Retrieval and Multi-scale Validation of Soil Moisture from Multi-temporal SAR Data in a Semi-Arid Tropical Region. Remote Sensing, 2015, 7, 8128-8153.	4.0	73
24	Comparison of SMOS and AMSR-E vegetation optical depth to four MODIS-based vegetation indices. Remote Sensing of Environment, 2016, 172, 87-100.	11.0	71
25	Global-scale surface roughness effects at L-band as estimated from SMOS observations. Remote Sensing of Environment, 2016, 181, 122-136.	11.0	69
26	Evaluation of SMOS, SMAP, ASCAT and Sentinel-1 Soil Moisture Products at Sites in Southwestern France. Remote Sensing, 2018, 10, 569.	4.0	68
27	Assimilation of SMOS soil moisture and brightness temperature products into a land surface model. Remote Sensing of Environment, 2016, 180, 292-304.	11.0	67
28	Comparison between SMOS Vegetation Optical Depth products and MODIS vegetation indices over crop zones of the USA. Remote Sensing of Environment, 2014, 140, 396-406.	11.0	66
29	Copula-Based Downscaling of Coarse-Scale Soil Moisture Observations With Implicit Bias Correction. IEEE Transactions on Geoscience and Remote Sensing, 2015, 53, 3507-3521.	6.3	60
30	Comparison of Dobson and Mironov Dielectric Models in the SMOS Soil Moisture Retrieval Algorithm. IEEE Transactions on Geoscience and Remote Sensing, 2015, 53, 3084-3094.	6.3	58
31	A sequential model for disaggregating near-surface soil moisture observations using multi-resolution thermal sensors. Remote Sensing of Environment, 2009, 113, 2275-2284.	11.0	56
32	SMOS soil moisture product evaluation over West-Africa from local to regional scale. Remote Sensing of Environment, 2015, 156, 383-394.	11.0	51
33	Testing regression equations to derive long-term global soil moisture datasets from passive microwave observations. Remote Sensing of Environment, 2016, 180, 453-464.	11.0	47
34	SMOS CATDS level 3 global products over land. Proceedings of SPIE, 2010, , .	0.8	46
35	A new calibration of the effective scattering albedo and soil roughness parameters in the SMOS SM retrieval algorithm. International Journal of Applied Earth Observation and Geoinformation, 2017, 62, 27-38.	2.8	44
36	Analysis of L-Band SAR Data for Soil Moisture Estimations over Agricultural Areas in the Tropics. Remote Sensing, 2019, 11, 1122.	4.0	43

#	Article	IF	CITATIONS
37	SMOS Retrieval Results Over Forests: Comparisons With Independent Measurements. IEEE Journal of Selected Topics in Applied Earth Observations and Remote Sensing, 2014, 7, 3858-3866.	4.9	42
38	An Analytical Model of Evaporation Efficiency for Unsaturated Soil Surfaces with an Arbitrary Thickness. Journal of Applied Meteorology and Climatology, 2011, 50, 457-471.	1.5	41
39	Modeling water needs and total irrigation depths of maize crop in the south west of France using high spatial and temporal resolution satellite imagery. Agricultural Water Management, 2017, 189, 123-136.	5.6	40
40	Mapping Dynamic Water Fraction under the Tropical Rain Forests of the Amazonian Basin from SMOS Brightness Temperatures. Water (Switzerland), 2017, 9, 350.	2.7	34
41	High resolution mapping of inundation area in the Amazon basin from a combination of L-band passive microwave, optical and radar datasets. International Journal of Applied Earth Observation and Geoinformation, 2019, 81, 58-71.	2.8	34
42	On the Use of Satellite Remote Sensing to Detect Floods and Droughts at Large Scales. Surveys in Geophysics, 2020, 41, 1461-1487.	4.6	33
43	MAPSM: A Spatio-Temporal Algorithm for Merging Soil Moisture from Active and Passive Microwave Remote Sensing. Remote Sensing, 2016, 8, 990.	4.0	31
44	Optimization of a Radiative Transfer Forward Operator for Simulating SMOS Brightness Temperatures over the Upper Mississippi Basin. Journal of Hydrometeorology, 2015, 16, 1109-1134.	1.9	29
45	An Initial Assessment of SMOS Derived Soil Moisture over the Continental United States. IEEE Journal of Selected Topics in Applied Earth Observations and Remote Sensing, 2012, 5, 1448-1457.	4.9	28
46	Stepwise Disaggregation of SMAP Soil Moisture at 100 m Resolution Using Landsat-7/8 Data and a Varying Intermediate Resolution. Remote Sensing, 2019, 11, 1863.	4.0	28
47	Comparison of SMOS and SMAP soil moisture retrieval approaches using tower-based radiometer data over a vineyard field. Remote Sensing of Environment, 2014, 154, 89-101.	11.0	27
48	Tradeâ€Offs Between 1â€Ð and 2â€Ð Regional River Hydrodynamic Models. Water Resources Research, 2020, 56, e2019WR026812.	4.2	27
49	Urban energy modeling and calibration of a coastal Mediterranean city: The case of Beirut. Energy and Buildings, 2019, 199, 223-234.	6.7	22
50	Considering combined or separated roughness and vegetation effects in soil moisture retrievals. International Journal of Applied Earth Observation and Geoinformation, 2017, 55, 73-86.	2.8	19
51	Estimation of daily CO2 fluxes and of the components of the carbon budget for winter wheat by the assimilation of Sentinel 2-like remote sensing data into a crop model. Geoderma, 2020, 376, 114428.	5.1	19
52	How much inundation occurs in the Amazon River basin?. Remote Sensing of Environment, 2022, 278, 113099.	11.0	18
53	Extracting Soil Water Holding Capacity Parameters of a Distributed Agro-Hydrological Model from High Resolution Optical Satellite Observations Series. Remote Sensing, 2016, 8, 154.	4.0	16
54	Snow observations in Mount Lebanon (2011–2016). Earth System Science Data, 2017, 9, 573-587.	9.9	16

#	Article	IF	CITATIONS
55	Soil Moisture Remote Sensing across Scales. Remote Sensing, 2019, 11, 190.	4.0	15
56	Impact of Demographic Growth on Seawater Intrusion: Case of the Tripoli Aquifer, Lebanon. Water (Switzerland), 2016, 8, 104.	2.7	12
57	Soil Moisture from Space. , 2016, , 3-27.		11
58	The Indian COSMOS Network (ICON): Validating L-Band Remote Sensing and Modelled Soil Moisture Data Products. Remote Sensing, 2021, 13, 537.	4.0	11
59	Salt water intrusion with heterogeneity and uncertainty: mathematical modeling and analyses. Developments in Water Science, 2004, 55, 1559-1571.	0.1	10
60	RFI in SMOS measurements: Update on detection, localization, mitigation techniques and preliminary quantified impacts on soil moisture products. , 2014, , .		10
61	Estimation of the L-Band Effective Scattering Albedo of Tropical Forests Using SMOS Observations. IEEE Geoscience and Remote Sensing Letters, 2017, 14, 1223-1227.	3.1	10
62	Denitrification and associated nitrous oxide and carbon dioxide emissions from the Amazonian wetlands. Biogeosciences, 2020, 17, 4297-4311.	3.3	9
63	A New L-Band Passive Radiometer For Earth Observation: SMOS-High Resolution (SMOS-HR). , 2020, , .		9
64	SMOS-NEXT: A New Concept for Soil Moisture Retrieval from Passive Interferometric Observations. EAS Publications Series, 2013, 59, 203-212.	0.3	8
65	Combining High-Resolution Remote Sensing Products with a Crop Model to Estimate Carbon and Water Budget Components: Application to Sunflower. Remote Sensing, 2020, 12, 2967.	4.0	8
66	Assessing the Contribution of Demographic Growth, Climate Change, and the Refugee Crisis on Seawater Intrusion in the Tripoli Aquifer. Water (Switzerland), 2018, 10, 973.	2.7	7
67	Hydrological Dynamics of the Congo Basin From Water Surfaces Based on Lâ€Band Microwave. Water Resources Research, 2021, 57, e2020WR027259.	4.2	7
68	Accuracy and Transferability of Artificial Neural Networks in Predicting in Situ Root-Zone Soil Moisture for Various Regions across the Globe. Water (Switzerland), 2020, 12, 3109.	2.7	6
69	Irrigation and Precipitation Hydrological Consistency with SMOS, SMAP, ESA-CCI, Copernicus SSM1km, and AMSR-2 Remotely Sensed Soil Moisture Products. Remote Sensing, 2020, 12, 3737.	4.0	6
70	Forecasting Sunflower Grain Yield by Assimilating Leaf Area Index into a Crop Model. Remote Sensing, 2020, 12, 3816.	4.0	6
71	Synergistic Calibration of a Hydrological Model Using Discharge and Remotely Sensed Soil Moisture in the ParanÃ; River Basin. Remote Sensing, 2021, 13, 3256.	4.0	4
72	Recent Improvements in the Dart Model for Atmosphere, Topography, Large Landscape, Chlorophyll		4

Fluorescence, Satellite Image Inversion. , 2020, , .

#	Article	IF	CITATIONS
73	Integrating process-related information into an artificial neural network for root-zone soil moisture prediction. Hydrology and Earth System Sciences, 2022, 26, 3263-3297.	4.9	4
74	Disaggregation as a top-down approach for evaluating 40 km resolution SMOS data using point-scale measurements: application to AACES-1. , 2010, , .		3
75	Model coupling for environmental flows, with applications in hydrology and coastal hydrodynamics. Houille Blanche, 2015, 101, 9-24.	0.3	3
76	Smos L-Band Vegetation Optical Depth is Highly Sensitive to Aboveground Biomass. , 2018, , .		3
77	Why To Model Remote Sensing Measurements In 3d? Recent Advances In Dart: Atmosphere, Topography, Large Landscape, Chlorophyll Fluorescence And Satellite Image Inversion. , 2020, , .		3
78	Event detection of hydrological processes with passive L-band data from SMOS. , 2010, , .		2
79	Soil Moisture Retrievals Based on Active and Passive Microwave Data. , 2016, , 351-378.		2
80	Dart: Radiative Transfer modeling for simulating terrain, airborne and satellite spectroradiometer and LIDAR acquisitions and 3D radiative budget of natural and urban landscapes. , 2016, , .		2
81	3D modeling of radiative transfer and energy balance in urban canopies combined to remote sensing acquisitions. , 2016, , .		2
82	Calibrating the effective scattering albedo in the SMOS algorithm: Some first results. , 2016, , .		2
83	Assessing Urban canopies 3D radiative and Energy Budgets with remote sensing and DART model. , 2017, , .		2
84	Global Weekly Inland Surface Water Dynamics from L-Band Microwave. , 2020, , .		2
85	Merging two passive microwave remote sensing (SMOS and AMSR_E) datasets to produce a long term record of Soil Moisture. , 2014, , .		1
86	Modeling specular reflectance and polarization in DART model for simulating remote sensing images of natural and urban landscapes. , 2016, , .		1
87	SMOS after six years in operations: First glance at climatic trends and anomalies. , 2016, , .		1
88	SWAF-HR: A High Spatial and Temporal Resolution Water Surface Extent Product Over the Amazon Basin. , 2018, , .		1
89	ls vegetation optical depth needed to estimate biomass from passive microwave radiometers? A statistical study using neural networks. , 2019, , .		1
90	Improvement of soil moisture and groundwater level estimations using a scaleâ€consistent river parameterization for the coupled ParFlow-CLM hydrological model: A case study of the Upper Rhine Basin. Journal of Hydrology, 2022, 610, 127991.	5.4	1

#	Article	IF	CITATIONS
91	SMOS L2 retrieval results over the American continent and comparisons with independent data sources. , 2013, , .		Ο
92	Compared performances of microwave passive soil moisture retrievals (SMOS) and active soil moisture retrievals (ASCAT) using land surface model estimates (MERRA-LAND). , 2014, , .		0
93	Performances of SMOS and AMSR-E soil moisture retrievals against Land Data Assimilation system estimates. , 2014, , .		0
94	First application of regression analysis to retrieve Soil Moisture from SMAP brightness temperature observations consistent with SMOS. , 2016, , .		0
95	Synergies Betwwen Smos and Sentinel-3. , 2018, , .		0
96	Analysis of L Band Radar Data Over Tropical Agricultural Areas. , 2019, , .		0
97	Daily Estimation of Inland Water Storage in the Madeira Basin During the Last Twenty Years (1998–2018). , 2021, , .		Ο
98	Global Assessment of Droughts in the Last Decade from SMOS Root Zone Soil Moisture. , 2021, , .		0